Table 4 Baseline characteristics of rheumatoid arthritis patients in the biological DMARDs group who did or did not meet criterion B for elevation of serum KL-6 levels

	Meeting criterion B (n = 27)	Not meeting criterion B (n = 124)
Gender (female) (%)	70.4	76.6
Mean age (years)	63.5 ± 9.7	58.1 ± 13.8
Mean disease duration (months)	100.6 ± 120.3	98.9 ± 108.4
Comorbidity		
Interstitial pneumonia (%)	44.4	27.4
Other pulmonary disease (%)	7.4	10.5
Past illness		
PCP (%)	0.0	0.0
Malignancy (%)	0.0	8.1
Drug-induced pulmonary disease (%)	0.0	2.4
Others (%)	37.0	22.6
Clinical characteristics		
Baseline KL-6 (U/ml)	419.5 ± 180.1	365.4 ± 373.3
MTX use at month 0 (%)	63.0	64.5
Mean dose of MTX at month 0 (mg/week)	8.3 ± 3.0	8.6 ± 2.5
Corticosteroid use at month 0 (%)	51.9	50.8
Mean dose of corticosteroid at month 0 (mg/day) (prednisolone equivalent)	6.5 ± 2.0	6.1 ± 3.6
DMARDs other than MTX use at month 0 (%)	22.2	25.8
Biological DMARDs-naïve (%)	92.6	74.2

Criterion B for elevation of serum KL-6 levels is defined in "Patients and methods" section

Values are mean ± SD, unless otherwise stated

RA rheumatoid arthritis, *PCP Pneumocystis jirovecii* pneumonia, *MTX* methotrexate, *DMARDs* disease-modifying antirheumatic drugs, *SD* standard deviation

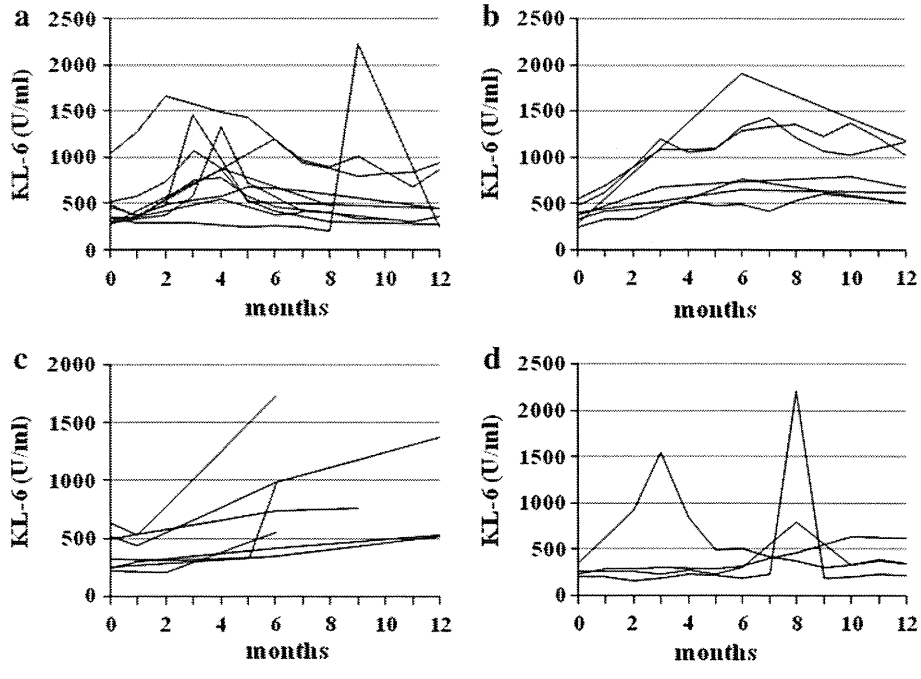

Fig. 1 Changes in serum KL-6 levels of rheumatoid arthritis patients meeting criterion B at least once during the observation period without apparent clinical events are shown. Data from the biological disease-modifying antirheumatic drugs (DMARDs) group: data from 10 patients meeting criterion R by month 12 (**a**), data from 7 patients not meeting criterion R by month 12 (**b**), and data from 7 patients without available data on serum KL-6 levels after meeting criterion B and reaching their maximum levels (**c**). **d** Data from the MTX group

combination of biological DMARDs and MTX. The percentages of patients with concomitant use of MTX were similar for patients who did and did not meet criterion B in the biological DMARDs group (63.0 versus 64.5 %) (Table 4). However, 5 (10.6 %) of 47 RA patients given MTX without biological DMARDs met criterion B (Table 2), and 4 (8.5 %) of these had any apparent reasons for the elevation of serum KL-6 levels. In our other study utilizing data from clinical trials [18], 3 (2.0 %) out of 149 patients given MTX + placebo met criterion B by week 24 or 28 without associated pulmonary events. These data indicate that we should consider potential contribution of MTX to the elevation of serum KL-6 levels during treatment with TNF inhibitor plus MTX.

A possible explanation for the elevation of serum KL-6 levels without apparent clinical events would be the presence of subclinical IP or PCP. We had 22 patients with serum levels of SP-D, another serum marker for interstitial lung disease [19], at both baseline and at least one additional time point, and we exploratory analyzed these data. Of the 22 patients, only two showed significant elevation of SP-D [defined as max. SP-D $\geq$110 ng/ml (upper limit of normal in Japan) and >1.5-fold from baseline] and both of these patients met criterion B. One of them developed PCP with simultaneous elevation of serum KL-6 and SP-D levels while he was receiving MTX without a biological DMARD. The other met criterion B without any pulmonary events 6 months after commencement of IFX with MTX and showed elevation of serum SP-D level 6 months after meeting criterion B. This patient did not have other available data for serum SP-D levels. Of the remaining 20 patients with serum SP-D levels reported, 5 patients met and 15 did not meet criterion B without significant elevation of SP-D. It appeared to be difficult to draw a definite conclusion from these data. In 20 of 33 patients who met criterion A in the biological DMARDs group, serum levels of β-D-glucan, a marker for PCP [15], were measured at the time of the elevation of serum KL-6 levels (data not shown), but did not increase throughout the observation period. These data suggest that subclinical PCP has a relatively low possibility of being the reason for the elevation of serum KL-6 levels.

In the normal state, bronchiolar epithelial cells and bronchial gland cells, as well as type II alveolar epithelial cells, produce KL-6. When lung injury occurs, proliferation or regeneration of alveolar type II cells and increased alveolar–capillary permeability have been reported to be mechanisms for the elevation of serum KL-6 levels [20]. However, the relationship between these mechanisms and the use of biological DMARDs or MTX is unknown, and further pathophysiological studies will be required to clarify the mechanism for spontaneous elevation of serum KL-6 levels during treatment with these drugs.

In our study, patients treated with TNF inhibitors had higher incidence of elevation of serum KL-6 levels meeting criterion A or B than patients treated with TCZ (Table 3). Because we could not avoid selection bias and recall bias in our study, we deliberately did not perform further statistical analyses. Prospective studies or analysis of clinical trial data may help clarify whether abnormal elevation of serum KL-6 levels is more frequently observed in patients given TNF inhibitors than in those given other classes of biological DMARDs.

How should rheumatologists manipulate treatment for RA patients given biological DMARDs when their serum KL-6 levels are elevated in clinical practice? Taking the established evidence for KL-6 into account, rheumatologists initially should compare chest X-ray or thoracic CT at baseline and at elevation of serum KL-6 levels and search for reasons for the elevation, such as PCP, IP, and malignancy. When these adverse events are not identified, continuing treatment with biological DMARDs under careful observation is a reasonable option for RA patients who have shown good responses to the treatments.

In summary, serum KL-6 levels may increase without associated clinical conditions in patients receiving biological DMARDs or MTX. Spontaneous reduction of serum KL-6 levels was observed in the majority of these patients; therefore continuing treatment with biological DMARDs under careful observation is a reasonable option in this clinical situation.

Acknowledgments This work was supported by a grant-in-aid from the Ministry of Health, Labor, and Welfare, Japan (H23-meneki-sitei-016 to M.H. and N.M.), by a grant-in-aid for scientific research from the Japan Society for the Promotion of Science (No. 23590171 to M.H. and N.M.), and the grant from the Japanese Ministry of Education, Global Center of Excellence (GCOE) Program, International Research Center for Molecular Science in Tooth and Bone Diseases (to N.M.). We would like to thank Ms. Ryoko Sakai for her contribution to the data analyses and Ms. Marie Yajima for her contribution to manuscript preparation.

Conflict of interest The Ad Hoc Committee for Safety of Biologics of the Japan College of Rheumatology did not receive any financial support from industry and independently investigated and discussed the issues and prepared this manuscript. T.A. has received research grants from Chugai Pharmaceutical and Takeda Pharmaceutical. H.K. has received honoraria from Abbott, Mitsubishi Tanabe Pharma Corporation, and Pfizer. Y.S. has received consultant fee from Abbott. T.K. has received consultancies, speaking fees, and honoraria from Abbott, Bristol Myers Squibb, Chugai Pharmaceutical, Eisai Pharmaceutical, Mitsubishi Tanabe Pharma Corporation, Takeda Pharmaceutical, Pfizer, and Otsuka Pharmaceutical. N.M. has received research grants from Abbott, Astellas Pharmaceutical Banyu Pharmaceutical, Chugai Pharmaceutical, Daiichi Sankyo Pharmaceutical, Eisai Pharmaceutical, Janssen Pharmaceutical, Mitsubishi Tanabe Pharma Corporation, Takeda Pharmaceutical, and Teijin Pharmaceutical. M.H. has received research grants from Abbott, Bristol

Myers Squibb, Chugai Pharmaceutical, Eisai Pharmaceutical, Janssen Pharmaceutical, Mitsubishi Tanabe Pharma Corporation, Takeda Pharmaceutical, and Pfizer and received consultant fees from Abbott, Bristol Myers Squibb, Chugai Pharmaceutical, and Janssen Pharmaceutical.

References

1. Takeuchi T, Tatsuki Y, Nogami Y, Ishiguro N, Tanaka Y, Yamanaka H, et al. Postmarketing surveillance of the safety profile of infliximab in 5000 Japanese patients with rheumatoid arthritis. Ann Rheum Dis. 2008;67:189–94.
2. Koike T, Harigai M, Inokuma S, Inoue K, Ishiguro N, Ryu J, et al. Postmarketing surveillance of the safety and effectiveness of etanercept in Japan. J Rheumatol. 2009;36:898–906.
3. Koike T, Harigai M, Ishiguro N, Inokuma S, Takei S, Takeuchi T, et al. Safety and effectiveness of adalimumab in Japanese rheumatoid arthritis patients: postmarketing surveillance report of the first 3,000 patients. Mod Rheumatol Japan Rheum Assoc. 2011.
4. Koike T, Harigai M, Inokuma S, Ishiguro N, Ryu J, Takeuchi T, et al. Postmarketing surveillance of tocilizumab for rheumatoid arthritis in Japan: interim analysis of 3881 patients. Ann Rheum Dis. 2011;70:2148–51.
5. Koike R, Takeuchi T, Eguchi K, Miyasaka N. Update on the Japanese guidelines for the use of infliximab and etanercept in rheumatoid arthritis. Mod Rheumatol. 2007;17:451–8.
6. Koike R, Harigai M, Atsumi T, Amano K, Kawai S, Saito K, et al. Japan College of Rheumatology 2009 guidelines for the use of tocilizumab, a humanized anti-interleukin-6 receptor monoclonal antibody, in rheumatoid arthritis. Mod Rheumatol. 2009;19:351–7.
7. Japan College of Rheumatology. Guideline for the use of TNF inhibitors in rheumatoid arthritis, Japan College of Rheumatology. Tokyo 2010 (in Japanese). http://www.ryumachi-jp.com/info/guideline_TNF_100930.html (updated 30-09-2010; cited 01-11-2011).
8. Japan College of Rheumatology. Guideline for the use tocilizumab in rheumatoid arthritis, Japan College of Rheumatology (in Japanese). 2010. http://www.ryumachi-jp.com/info/guideline_TCZ_100716.html (updated 16-07-2010).
9. Stahel RA, Gilks WR, Lehmann HP, Schenker T. Third International Workshop on Lung Tumor and Differentiation Antigens: overview of the results of the central data analysis. Int J Cancer Suppl. 1994;8:6–26.
10. Kohno N, Awaya Y, Oyama T, Yamakido M, Akiyama M, Inoue Y, et al. KL-6, a mucin-like glycoprotein, in bronchoalveolar lavage fluid from patients with interstitial lung disease. Am Rev Respir Dis. 1993;148:637–42.
11. Miyata M, Sakuma F, Fukaya E, Kobayashi H, Rai T, Saito H, et al. Detection and monitoring of methotrexate-associated lung injury using serum markers KL-6 and SP-D in rheumatoid arthritis. Intern Med. 2002;41:467–73.
12. Nakajima H, Harigai M, Hara M, Hakoda M, Tokuda H, Sakai F, et al. KL-6 as a novel serum marker for interstitial pneumonia associated with collagen diseases. J Rheumatol. 2000;27:1164–70.
13. Nakamura H, Tateyama M, Tasato D, Haranaga S, Yara S, Higa F, et al. Clinical utility of serum beta-D-glucan and KL-6 levels in *Pneumocystis jirovecii* pneumonia. Intern Med. 2009;48:195–202.
14. Ohnishi H, Yokoyama A, Yasuhara Y, Watanabe A, Naka T, Hamada H, et al. Circulating KL-6 levels in patients with drug induced pneumonitis. Thorax. 2003;58:872–5.
15. Tasaka S, Hasegawa N, Kobayashi S, Yamada W, Nishimura T, Takeuchi T, et al. Serum indicators for the diagnosis of pneumocystis pneumonia. Chest. 2007;131:1173–80.
16. Takeuchi T, Miyasaka N, Inoue K, Abe T, Koike T. Impact of trough serum level on radiographic and clinical response to infliximab plus methotrexate in patients with rheumatoid arthritis: results from the RISING study. Mod Rheumatol Japan Rheum Assoc. 2009;19:478–87.
17. Arnett FC, Edworthy SM, Bloch DA, McShane DJ, Fries JF, Cooper NS, et al. The American Rheumatism Association 1987 revised criteria for the classification of rheumatoid arthritis. Arthritis Rheum. 1988;31:315–24.
18. Harigai M, Takamura A, Atsumi T, Dohi M, Hirata S, Kameda H, et al. Elevation of KL-6 serum levels in clinical trials of tumor necrosis factor inhibitors in patients with rheumatoid arthritis—a report from the ad-hoc committee for safety of biological DAMRDs of the Japan College of Rheumatology. 2012 (submitted).
19. van den Blink B, Wijsenbeek MS, Hoogsteden HC. Serum biomarkers in idiopathic pulmonary fibrosis. Pulm Pharmacol Ther. 2010;23:515–20.
20. Oyama T, Kohno N, Yokoyama A, Hirasawa Y, Hiwada K, Oyama H, et al. Detection of interstitial pneumonitis in patients with rheumatoid arthritis by measuring circulating levels of KL-6, a human MUC1 mucin. Lung. 1997;175:379–85.

Laboratory Investigation (2013) 93, 72–80

Overexpression of TNF-α-converting enzyme in fibroblasts augments dermal fibrosis after inflammation

Shinji Fukaya[1,2,*], Yuki Matsui[3,*], Utano Tomaru[1], Ai Kawakami[3], Sayuri Sogo[4], Toshiyuki Bohgaki[2], Tatsuya Atsumi[2], Takao Koike[2], Masanori Kasahara[1] and Akihiro Ishizu[5]

TNF-α-converting enzyme (TACE) can cleave transmembrane proteins, such as TNF-α, TNF receptors, and epidermal growth factor receptor (EGFR) ligands, to release the extracellular domains from the cell surface. Recent studies have suggested that overexpression of TACE may be associated with the pathogenesis of inflammation and fibrosis. To determine the roles of TACE in inflammation and fibrosis, TACE transgenic (TACE-Tg) mice, which overexpressed TACE systemically, were generated. As the transgene-derived TACE was expressed as an inactive form, no spontaneous phenotype developed in TACE-Tg mice. However, the transgene-derived TACE could be converted to an active form by furin *in vitro* and by phorbol myristate acetate (PMA) *in vivo*. Subcutaneous injection of PMA into mice induced inflammatory cell infiltration 1 day later and subsequent dermal fibrosis 7 days later. Interestingly, the degree of dermal fibrosis at day 7 was significantly higher in TACE-Tg mice than in wild-type mice. Correspondingly, PMA increased the expression of type I collagen in the primary culture of dermal fibroblasts derived from TACE-Tg mice. Furthermore, phosphorylated EGFR was increased in the fibroblasts by the PMA treatment. The collective findings suggest that TACE overexpression and activation in fibroblasts could shed off putative EGFR ligands. Subsequently, the soluble EGFR ligands could bind and activate EGFR on fibroblasts, and then increase the type I collagen expression resulting in induction of dermal fibrosis. These results also suggest that TACE and EGFR on fibroblasts may be novel therapeutic targets of dermal fibrosis, which is induced after diverse inflammatory disorders of the skin.
Laboratory Investigation (2013) **93,** 72–80; doi:10.1038/labinvest.2012.153; published online 12 November 2012

KEYWORDS: EGFR; fibrosis; inflammation; PMA; TACE

TNF-α-converting enzyme (TACE), which belongs to a disintegrin and metalloproteinase (ADAM) family, can cleave transmembrane proteins to release the extracellular domains from the cell surface.[1,2] Initially produced as an inactive 120 kDa protein, the N-terminus prodomain is removed by furin at the trans-golgi network, and consequently TACE is converted to an active form of 100 kDa protein.[3–6] The active form of TACE is transported to the plasma membrane and binds to its substrates on the cell surface. Substrates of TACE include TNF-α, TNF receptors, and epidermal growth factor receptor (EGFR) ligands.

When focusing on the role of TNF-α in inflammation, it is considered that TACE contributes to promote inflammation by increasing soluble TNF-α. However, it is also considered that TACE plays a role in the suppression of inflammation by decreasing membrane-type TNF receptors and producing soluble TNF receptors, which can work as decoy receptors. These concepts seem contradictory, but TACE really functions to maintain the physiological homeostasis. The expression of TACE substrates is strictly regulated in a time-dependent manner during the inflammation process.

On the other hand, it has been demonstrated that rat collagen antibody-induced arthritis and lipopolysaccharide (LPS)-induced acute lung injury can be treated by TACE inhibitors.[7,8] Recently, Terao *et al*[9] have demonstrated that murine bleomycin-induced scleroderma could also be treated by TACE inhibitors. These findings suggest that TACE may be critically involved in the pathogenesis of these inflammatory

[1]Department of Pathology, Hokkaido University Graduate School of Medicine, Sapporo, Japan; [2]Department of Internal Medicine II, Hokkaido University Graduate School of Medicine, Sapporo, Japan; [3]Graduate School of Health Sciences, Hokkaido University, Sapporo, Japan; [4]School of Health Sciences, Hokkaido University, Sapporo, Japan and [5]Faculty of Health Sciences, Hokkaido University, Sapporo, Japan
Correspondence: Professor A Ishizu, MD, PhD, Faculty of Health Sciences, Hokkaido University Kita-12, Nishi-5, Kita-ku, Sapporo Hokkaido 060-0812, Japan.
E-mail: aishizu@med.hokudai.ac.jp
*These authors contributed equally to this work.

Received 17 January 2012; revised 19 September 2012; accepted 25 September 2012

and fibrous connective tissue diseases. However, the precise mechanism of the implication of TACE in inflammation and fibrosis has not been revealed. This study aimed to clarify the role of TACE in the pathogenesis of inflammation and fibrosis using TACE transgenic (TACE-Tg) mice, which could overexpress TACE in the systemic organs.

MATERIALS AND METHODS

Generation of TACE-Tg Mice

The transgene for generation of TACE-Tg mice contained the full-length mouse TACE cDNA, which connected the Flag tag to the 3′ region. The connection of the Flag tag rendered distinction of the transgene-derived TACE from the endogenous TACE. The construct was inserted into pCAGGS vector containing the β-actin promoter, which could bring systemic expression of the transgene. Then, the pCAGGS vector carrying the transgene was microinjected into fertilized eggs of BDF1 mice at Genome Information Research Center, Research Institute of Microbial Disease, Osaka University (Osaka, Japan). Four founder mice obtained were mated with C57BL/6 mice (Japan Clea, Tokyo, Japan), and then the offspring mice were backcrossed into C57BL/6 mice more than 6 times. Among them, one stable line of TACE-Tg mice with heterozygous transgene insertion was served for this study. Age-matched wild-type (WT) C57BL/6 mice were used for the control. Experiments using mice were done in accordance with the guidelines for the care and use of laboratory animals in Hokkaido University.

Real-Time RT-PCR

For RNA extraction from mouse tissues, RNeasy Mini kit (Qiagen, Hilden, Germany) was used. After digestion of contaminated genomic DNA by DNase I, RNA was reverse transcribed to cDNA using Superscript III First-Strand Synthesis System (Invitrogen, Carlsbad, CA, USA). The expression of TACE mRNA was quantified by real-time RT-PCR using QuantiTect SYBR Green PCR kit (Qiagen). The primer sequences for TACE were as follows: 5′-ATCTG AAGAGTTTGTTCGTCGAG-3′ (sense) and 5′-TCCACGG CCCATGTATTTAT-3′ (antisense). PCR was run on ABI Prism 7000 (Applied Biosystems, Carlsbad, CA, USA) as follows: after denaturation at 95 °C for 10 min, 40 cycles of reaction at 95 °C for 15 s and at 56 °C for 60 s were carried out. For the internal control, the expression of hypoxanthine-guanine phosphoribosyltransferase 1 (HPRT1) was monitored. The primer sequences for HPRT-1 were as follows: 5′-TGGAAAGAATGTCTTGATTGTTGAA-3′ (sense) and 5′-AGCTTGCAACCTTAACCATTTTG-3′ (antisense).

Western Blotting

The mouse tissues were homogenized in lysis buffer (0.1% sodium dodecyl sulfate (SDS), 1% Nonidet-P40, 0.5% sodium deoxycholate, 100 μg/ml phenylmethylsulfonyl fluoride, 1 mM sodium orthovanadate, protease inhibitor cocktail (Complete Mini, Roche, Basel, Switzerland)). The lysates adjusted ranging from 10 to 40 μg/lane were fractionated on 7.5% SDS polyacrylamide gel and then transferred onto PVDF membranes (GE Healthcare, Buckinghamshire, UK). After blocking by TBS-T (0.1% Tween-20 in Tris-buffered saline) containing 2% non-fat milk, the membranes were incubated with 1:5000 dilution of the anti-TACE antibody (Santa Cruz Biotechnology, Santa Cruz, CA, USA) or 1:5000 dilution of the anti-Flag antibody (Sigma-Aldrich, St Louis, MO, USA) overnight at 4 °C. After 3 times of wash by TBS-T, the membranes were next incubated with 1:25 000 dilution of the peroxidase-labeled secondary antibodies (GE Healthcare) overnight at 4 °C. Protein bands were detected using ECL Advance Western Blotting Detection kit (GE Healthcare). The anti-TACE antibody used in this study could react with the C-terminus of mouse TACE; thus, it could detect both the inactive and active forms.

Activation of TACE by Furin *In Vitro*

The skin tissues obtained from TACE-Tg and WT mice were lysed in the furin assay buffer (100 mM HEPES (pH 7.5), 0.5% Triton X-100, 1 mM $CaCl_2$, and 1 mM 2-mercaptoethanol). The lysates (140 μg/100 μl) were incubated with recombinant human furin (Sigma-Aldrich) at respective concentrations of 0, 0.1, and 1 unit/μl for 1 h at 30 °C. The samples were then fractionated on 7.5% SDS polyacrylamide gel, and western blotting was performed using the anti-TACE or anti-Flag antibodies.

Measurement of TACE Activity

The skin lysates treated by furin were subjected to measurement of TACE activity. The TACE activity was measured using SensoLyte 520 TACE Activity Assay kit (AnaSpec, Fremont, CA, USA) and Varioskan Flash Microplate Multimode Readers (Thermo Fisher Scientific, Waltham, MA, USA) according to the manufacturer's protocol.

Primary Culture of Dermal Fibroblasts

The back skin of TACE-Tg and WT mice were turned inside out and 3 mm pieces of the dermis were excised, put on flat dishes, and then incubated in RPMI-1640 (Sigma-Aldrich) containing 20% fetal calf serum, 50 μg/ml streptomycin, and 50 U/ml penicillin. Several days later, spindle-shaped cells migrated and proliferated around the skin pieces. After removal of the skin pieces, the cells were used as primary culture of dermal fibroblasts. Experiments were conducted using the cells at 3–5 passages.

Stimulation of Dermal Fibroblasts by PMA

The primary culture of dermal fibroblasts was stimulated by phorbol myristate acetate (PMA; LC Laboratories, Woburn, MA, USA) at respective concentrations of 0, 6.4, 64, and 640 nM. After 30 min of incubation at 37 °C, the cells were lysed, and then the lysates were served for the anti-TACE or anti-Flag immunoblotting.

Subcutaneous Injection of PMA

TACE-Tg and WT mice (10 weeks old, female) with shaved back skin were subcutaneously injected with 0.08 μg PMA in 0.1 ml PBS (1300 nM) using 29 G syringe needle. As control, the same volume of PBS without PMA was injected subcutaneously.

Histological Evaluation

At 1 and 7 days after the inoculation, the skin sites with PMA and PBS injections were excised as 6 mm round-shaped pieces, fixed in formalin, and then subjected to hematoxylin and eosin (HE) staining. The samples at 7 days were also subjected to Elastica–Masson (EM) staining. Dermal thickening ratio was calculated as follows: (1) thickness of dermis was measured at three random points of the sites with PBS injection, (2) mean thickness at the sites with PBS injection was calculated, (3) thickness of dermis was measured at three random points of the sites with PMA injection, and (4) dermal thickness ratios were calculated by dividing the thickness of dermis at the PMA injection sites by the mean dermal thickness at the sites with PBS injection.

Expression of Type I Collagen

To evaluate fibrosis in the molecular level, the expression of type I collagen (collagen 1A1) was examined by real-time RT-PCR. First, at 7 days, the skin sites with PMA and PBS injections were excised as 6 mm round-shaped pieces, RNA was extracted from the tissues, and then real-time RT-PCR was performed as described above. The primers for collagen 1A1 were as follows: 5′-GAGCCCTCGCTTCCGTACTC-3′ (sense) and 5′-TGTTCCCTACTCAGCCGTCTGT-3′ (antisense). Next, the primary culture of dermal fibroblasts was treated by PMA at respective concentrations of 0, 20, 160, and 1300 nM. After 4 h of incubation at 37 °C, RNA was extracted from the cells, and then the expression of collagen 1A1 was examined similarly by real-time RT-PCR.

TACE Inhibition Assay

The fibroblasts derived from TACE-Tg mice were treated by 1300 nM of PMA with or without 25 μg/ml of TAPI-0 (Enzo Life Sciences, Farmingdale, NY, USA) at 37 °C. TAPI-0 can inhibit TACE and other matrixmetalloproteases.[10] The concentration of TAPI-0 was adopted according to the literature.[11] After 4 h of incubation, RNA was extracted from the cells, and then the expression of collagen 1A1 was examined by real-time RT-PCR as described above.

Detection of Phosphorylated EGFR

To determine if EGFR was activated by PMA, phosphorylation of EGFR was examined. The primary culture of dermal fibroblasts was treated by PMA at respective concentrations of 0, 20, 160, and 1300 nM. After 1 h of incubation at 37 °C, RNA and cell lysates were extracted. The RNA was then served for RT-PCR using the EGFR primers (sense: 5′-GAACTGGGCTTAGGGAACTGC-3′, antisense: 5′-CATTGG GACAGCTTGGATCAC-3′), and the lysates were served for western blotting using the anti-phosphorylated EGFR antibody (Phospho-EGF Receptor (Tyr1068); Cell Signaling Technology, Tokyo, Japan). RT-PCR was carried out as described above. As internal controls, the expression of HPRT1 and the amount of actin detected by the anti-actin antibody (Chemicon International, Temecula, CA, USA) were monitored.

Statistics

Data were presented as mean ± s d. Student's *t*-test was applied for statistical analysis. The *P*-value of <0.05 was considered to be significant.

RESULTS

Overexpression of TACE in TACE-Tg Mice

The TACE mRNA and protein expressions in the systemic organs of 6-week-old TACE-Tg and WT mice were evaluated by real-time RT-PCR and western blotting, respectively. The TACE mRNA expression in all organs examined was higher in TACE-Tg mice than in WT mice, although the expression level was variable among organs (Figure 1a). The top five organs with the highest level of expression of TACE mRNA included the muscle, pancreas, heart, skin, and intestine. In WT mice, the TACE mRNA expression was relatively high in the pancreas and skin. The TACE protein expression, which was detected by the anti-TACE immunoblotting, well reflected the mRNA expression (Figure 1b). These findings

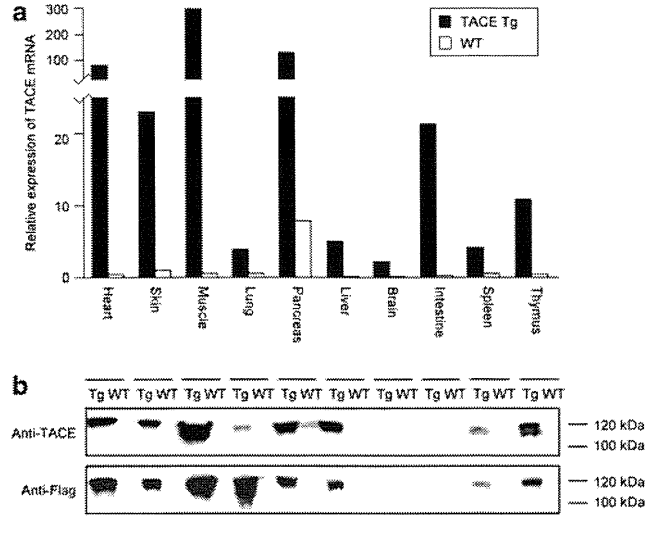

Figure 1 TACE mRNA and protein expressions in TACE-Tg and WT mice. The mRNA expressions of TACE in systemic organs of 6-week-old TACE-Tg and WT mice were quantified using real-time RT-PCR (**a**). The expression level in each organ was standardized by the level in the skin of WT mice. The expression of TACE protein was examined by western blotting (**b**). Lysates of systemic organs from 6-week-old TACE-Tg and WT mice were subjected to anti-TACE and anti-Flag immunoblotting. Experiments were repeated 3 times, and similar results were reproduced. Representative data are shown.

indicated the overexpression of TACE in TACE-Tg mice compared with WT mice. The anti-Flag immunoblotting suggested that the difference in the amount of TACE between TACE-Tg and WT mice was attributable to the expression of the transgene-derived TACE. Remarkably, most of the transgene-derived TACE protein was detected as the 120 kDa inactive form.

No Spontaneous Phenotype in TACE-Tg Mice

Comparison of histology of systemic organs between 6-week-old TACE-Tg mice and WT mice revealed no remarkable difference (Supplementary Figure 1). The TACE-Tg mice kept for up to 2 years showed no spontaneous development of a specific phenotype. This might be consistent with the presence of most of all transgene-derived TACE protein as the inactive form in TACE-Tg mice.

Activation of TACE by Furin

ADAM family molecules, including TACE, undergo proteolysis to the active form by protein convertases.[3,4] The inactive TACE of 120 kDa protein is removed in the N-terminus prodomain and then converted to the active form of 100 kDa protein by furin *in vivo*.[5,6] To determine the catalytic capacity of transgene-derived TACE, the tissue lysates of skin from TACE-Tg and WT mice were incubated with furin *in vitro*. The western blotting using the anti-TACE and anti-Flag antibodies revealed that the transgene-derived TACE protein could be converted to the 100 kDa active form by furin in a dose-dependent manner (Figure 2a). Compatible with these findings, the TACE activity in the samples from TACE-Tg mice was increased by furin dose-dependently, and the increased TACE activities in the samples from TACE-Tg mice exhibited significantly higher levels than those in WT samples (Figure 2b).

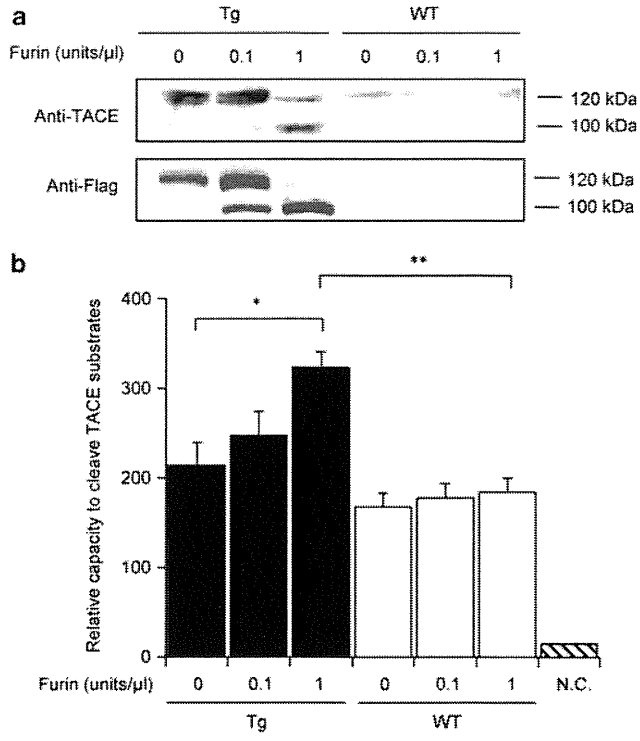

Figure 2 TACE activation by furin *in vitro*. Lysates of the skin from 6-week-old TACE-Tg and WT mice were incubated with furin at respective concentrations of 0, 0.1, and 1 unit/μl for 1 h at 30 °C. The samples were then subjected to anti-TACE and anti-Flag immunoblotting (**a**). Experiments were repeated 3 times, and similar results were reproduced. Representative data are shown. TACE activities in the samples (TACE-Tg: $n=3$, WT: $n=3$) were measured using SensoLyte 520 TACE Activity Assay kit (**b**). NC represents the spontaneous cleavage of TACE substrates in the kit. $^{*}P<0.05$, $^{**}P<0.01$.

Activation of TACE by PMA *In Vitro*

Administration of furin into mice is difficult because furin exclusively functions in the cytoplasm *in vivo*. In this study, alternative stimulation, which can convert TACE to the active form, was sought; hence, PMA was employed. When the primary culture of dermal fibroblasts was stimulated by PMA, the transgene-derived TACE protein was effectively converted to the active form (Figure 3a). Although the TACE activity in WT fibroblasts was significantly increased by PMA dose-dependently as well as that in the TACE-Tg fibroblasts, the increased amount of active TACE in WT samples seemed to remain at an undetectable level of the anti-TACE immunoblotting (Figure 3b).

Activation of TACE by PMA *In Vivo*

To determine that PMA could convert TACE to the active form *in vivo*, PMA was subcutaneously injected into TACE-Tg and WT mice, and then skin samples were obtained 1 and 7 days after the inoculation. Western blotting using the anti-TACE and anti-Flag antibodies revealed that the active TACE of 100 kDa protein increased in the sites of PMA injection in TACE-Tg mice at day 1. The amount of the active TACE in the sites of PMA injection in WT mice did not reach detection level (Figure 4a). The TACE activation recovered to the unstimulated level at 7 days after the PMA injection even in TACE-Tg mice. The TACE activity in the skin tissues of WT mice was significantly increased by PMA at day 1 as well as that in the TACE-Tg samples, although the increased amount of active TACE in the WT samples still remained at an undetectable level of the anti-TACE immunoblotting (Figure 4b).

Augmented Dermal Fibrosis after PMA-Induced Inflammation in TACE-Tg Mice

At 1 day after PMA injection, a severe infiltration of polymorphonuclear cells was observed in the subcutaneous tissue. Variety and degree of inflammatory cell infiltration were equivalent between TACE-Tg and WT mice (Figure 5). Thickening of the dermis and scar formation in the subcutaneous tissue were observed at the inflammation sites 7 days after the PMA injection (Figures 6a–h). The dermal thickening ratio (PMA injection site/PBS injection site) was significantly higher in TACE-Tg mice than in WT mice

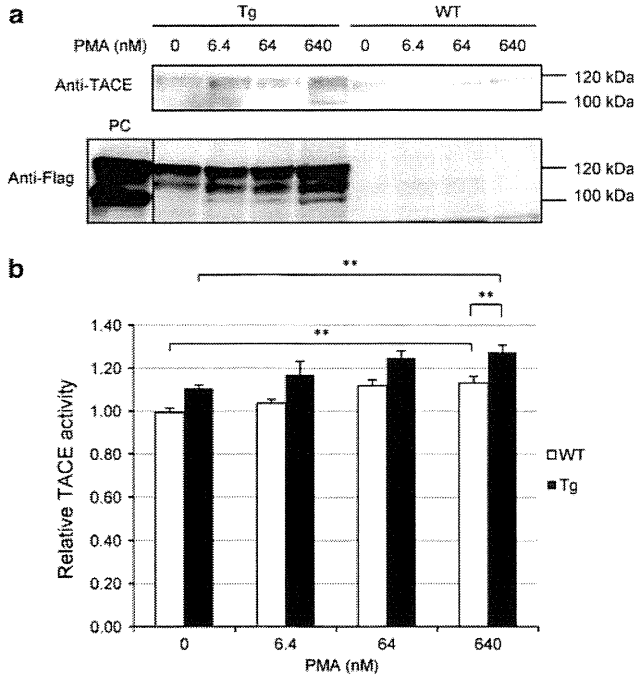

Figure 3 TACE activation by PMA *in vitro*. The primary culture of dermal fibroblasts derived from TACE-Tg and WT mice was stimulated by PMA at respective concentrations of 0, 6.4, 64, and 640 nM. After 30 min of incubation at 37 °C, the cells were lysed, and then the lysates were subjected to anti-TACE and anti-Flag immunoblotting (**a**). Experiments were repeated 3 times, and similar results were reproduced. Representative data are shown. PC: positive control (furin-treated TACE-Tg skin lysates used in Figure 2). TACE activity in each sample ($n = 3$, in each group) was measured using SensoLyte 520 TACE Activity Assay kit (**b**). $^{**}P < 0.01$.

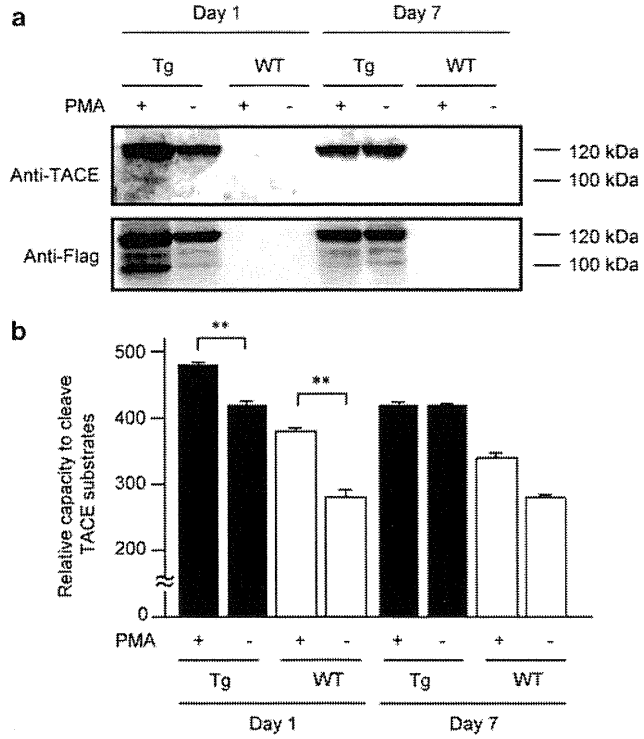

Figure 4 TACE activation by PMA *in vivo*. PMA (0.08 μg/0.1 ml PBS, 1300 nM) was injected subcutaneously into TACE-Tg and WT mice using 29 G syringe needle. As a control, the same volume of PBS without PMA was injected subcutaneously. Lysates were obtained from the sites with PMA and PBS injection, respectively, at day 1 and day 7. Western blotting was performed using the anti-TACE and anti-Flag antibodies (**a**). Experiments were repeated 3 times, and similar results were reproduced. Representative data are shown. TACE activity in each sample ($n = 3$, in each group) was measured using SensoLyte 520 TACE Activity Assay kit (**b**). $^{**}P < 0.01$.

(Figure 6i). Correspondingly, the mRNA expression of type I collagen in the skin 7 days after the PMA injection was relatively higher in TACE-Tg mice than in WT mice, though there was no statistical significant difference (Figure 6j). Notably, the type I collagen expression at the sites of PMA injection reached twofold level of the PBS-injected sites in TACE-Tg mice, whereas the expression at PMA injection sites was equal to that of the PBS injection sites in WT mice.

Induction of Type I Collagen Expression in Dermal Fibroblasts by PMA

To elucidate the hypothesis that the quantitative difference of TACE in dermal fibroblasts between TACE-Tg and WT mice was attributable to the degree of dermal fibrosis after the PMA-induced inflammation, the primary culture of dermal fibroblasts was stimulated by PMA *in vitro*, and then the mRNA expression of type I collagen was examined by real-time RT-PCR. As a result, the levels of type I collagen expression were upregulated by PMA dose-dependently in dermal fibroblasts of TACE-Tg mice, although the expression was not altered by the PMA treatment in dermal fibroblasts of WT mice (Figure 7a). In addition, the induction of type I collagen by PMA was significantly inhibited by the TACE inhibitor, TAPI-0 (Figure 7b). These findings suggested that the overexpression and activation of TACE in dermal fibroblasts could promote the type I collagen expression.

Increase of Phosphorylated EGFR in Dermal Fibroblasts by PMA

It has been shown that the expression of type I collagen was driven by the EGFR signal in fibroblasts.[12] To determine the activation of EGFR, the primary culture of dermal fibroblasts was treated by PMA, and then the expressions of EGFR and phosphorylated EGFR were examined. As a result, phosphorylated EGFR was increased by the PMA treatment dose-dependently, and the degree was higher in TACE-Tg mice than in WT mice (Figure 7c).

DISCUSSION

Association of the TACE expression with the pathogenesis of inflammation and fibrosis has been documented in animal models.[7–9] In humans, TACE has also been demonstrated to be involved in the pathogenesis of inflammatory and fibrous connective tissue diseases, such as rheumatoid arthritis[13,14] and systemic sclerosis (SSc).[15] Bohgaki *et al*[15] reported that TACE was overexpressed in peripheral blood monocytes of

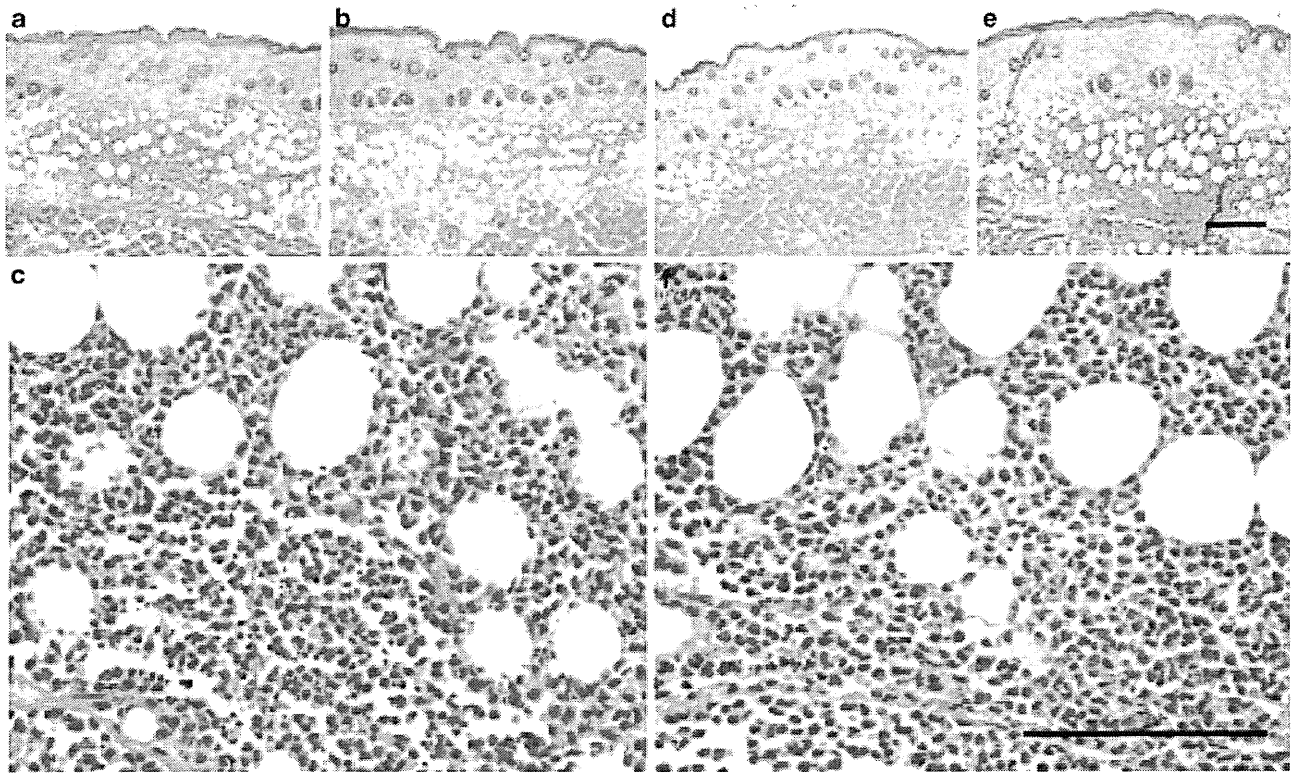

Figure 5 Subcutaneous inflammatory cell infiltration at sites with PMA injection At 1 day after the PMA injection, the sites with PMA injection were excised from TACE-Tg ($n=5$) and WT ($n=8$) mice, and then subjected to HE staining (**a**, **b**, **c**: TACE-Tg; **d**, **e**, **f**: WT; bar: 100 μM). Representative photos are shown.

patients with early stage of SSc, and that the TACE expression was decreased by treatment. These findings suggest that the overexpression of TACE in monocytes might be critically implicated in the development of SSc. On the other hand, it remains elusive how TACE in organ cells can be implicated in the pathogenesis of inflammation and fibrosis.

In the present study, TACE-Tg mice were generated in order to answer the question (Figure 1). As a majority of the transgene-derived TACE were expressed as an inactive form, no spontaneous phenotype occurred in TACE-Tg mice (Supplementary Figure 1). However, furin could convert the transgene-derived inactive TACE to active form; thus, TACE-Tg mice were regarded as inducible models of TACE overexpression and activation (Figure 2). Interestingly, furin failed to activate endogenous TACE unlike the transgene-derived TACE. Although the reason should be revealed by further studies, it is possible that undetermined factors in tissue lysates interfered with the measurement of TACE activity when inactive TACE were converted to active form in the tissue lysates. The amount of the putative inhibitory factors seemed to be enough to mask the TACE activity in WT samples mostly, but insufficient to mask that in TACE-Tg samples with overexpression of TACE.

As furin functions exclusively in the cytoplasm *in vivo*, we employed PMA as stimulant to induce TACE activation in TACE-Tg mice (Figure 3). As a result, the overexpression and activation of TACE in fibroblasts were demonstrated to augment dermal fibrosis after inflammation (Figures 4–6). The subcutaneous injection of PMA into TACE-Tg mice activated TACE in the tissue 1 day later and induced subsequent dermal fibrosis 7 days later. As PMA-induced activation of TACE already returned to the baseline level at day 7, it remained unclear whether the TACE overexpression and activation at day 1 were critically associated with the increased fibrosis at day 7. Although further studies are needed to clarify the association, it is possible that the TACE-dependent type I collagen induction at an early state in inflammation could make an orientation toward subsequent fibrosis. Interestingly, the degree of dermal fibrosis 7 days after PMA injection was significantly higher in TACE-Tg mice than in WT mice, although the degree of inflammatory cell infiltration at day 1 was comparable between the two. These findings suggest that the overexpression of TACE is related to fibrosis after inflammation rather than inflammation itself.

There is a controversy over the contribution of TACE to tissue fibrosis. Terao *et al*[9] demonstrated that TACE contributed to dermal fibrosis using murine bleomycin-induced scleroderma model. This finding corresponds to our results. On the contrary, Leco *et al*[16] reported that lung emphysema, an opposite phenotype of fibrosis, developed in tissue inhibitor of metalloproteinase 3 (TIMP-3)-deficient

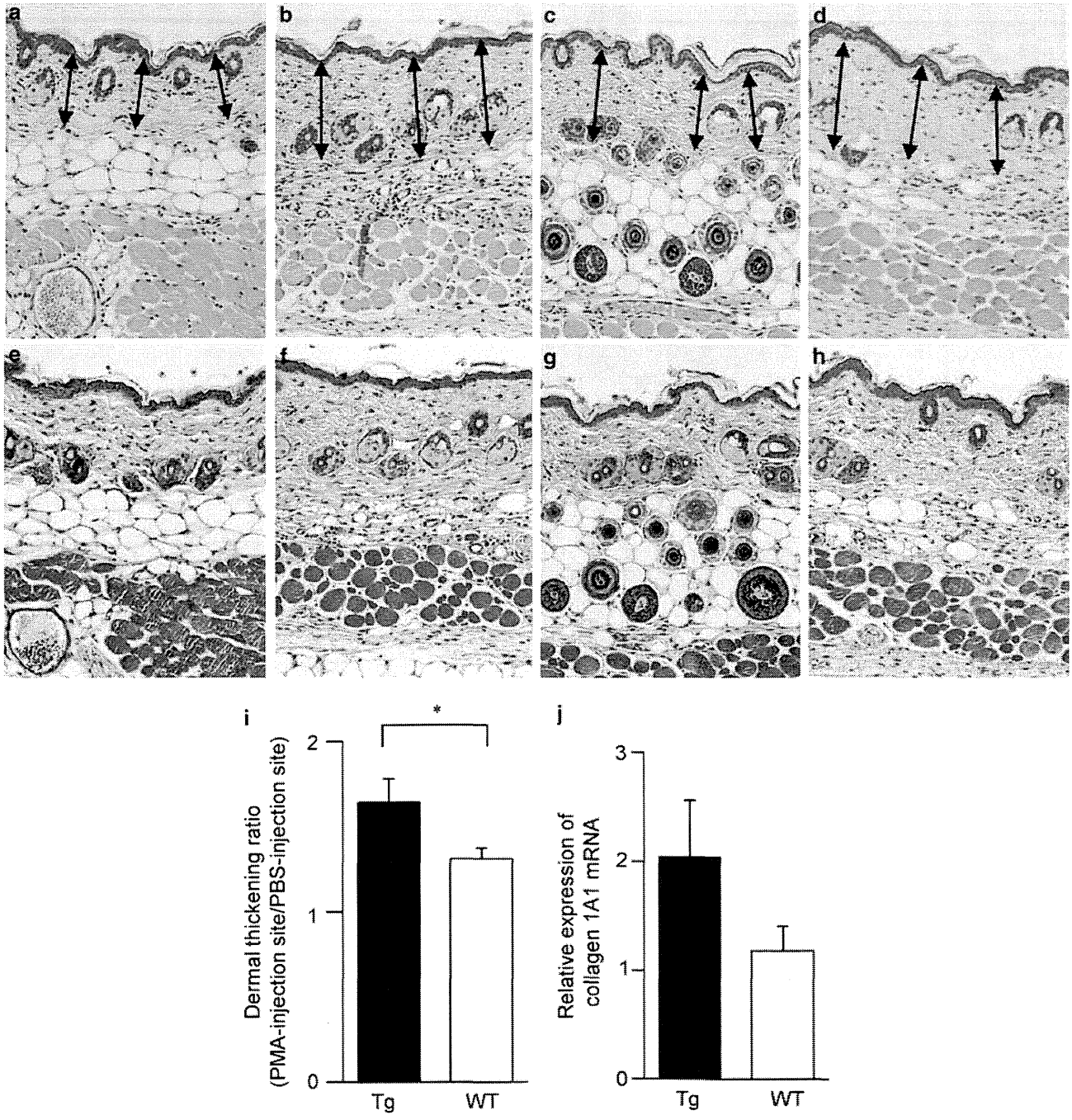

Figure 6 Dermal fibrosis at sites with PMA injection. At 7 days after the PMA injection, the sites with PMA injection (**b**, **d**, **f**, **h**) and the sites with PBS injection (**a**, **c**, **e**, **g**) were excised from TACE-Tg ($n=5$) and WT ($n=8$) mice, and then subjected to HE (**a**–**d**) and EM (**e**–**h**) staining (**a**, **b**, **e**, **f**: TACE-Tg, $n=5$; **c**, **d**, **g**, **h**: WT, $n=8$). Representative photos are shown. Dermal thickening ratios were calculated as follows: dermal thickness measured at three random points of the sites with PMA injection (arrows in **b** and **d**)/mean value of dermal thickness measured at three random points of the sites with PBS injection (arrows in **a** and **c**), and then were compared between TACE-Tg and WT mice (**i**). The skin tissues at sites with PMA and PBS injections were obtained at day 7, the expression of type I collagen (collagen 1A1) was examined by real-time RT-PCR, and then fold increase by the PMA injection was compared between TACE-Tg ($n=5$) and WT ($n=8$) mice (**j**). $^*P<0.05$.

mice. As TIMP-3 functions as a TACE inhibitor *in vivo*, TIMP-3-deficient mice have been documented as a TACE activation model.[17,18] Therefore, this finding suggests that TACE plays an opposite role in induction of tissue fibrosis and is contradictory to our results. However, TIMP-3-deficient mice are not necessarily an ideal model of TACE activation *in vivo* because TIMP-3 inhibits not only TACE but also other metalloproteinases.

To confirm the contribution of TACE overexpression in fibroblasts to dermal fibrosis, the expression of type I

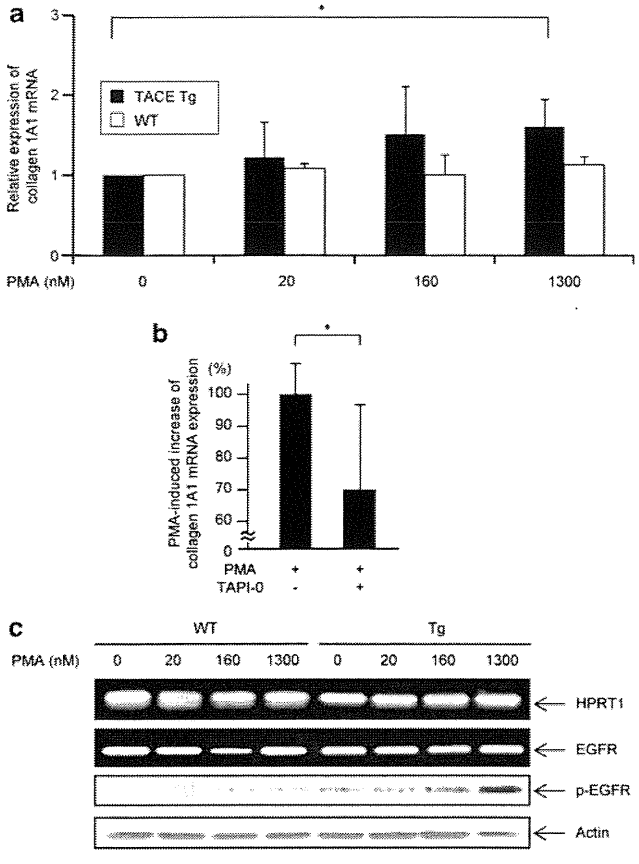

Figure 7 Increased type I collagen and phosphorylated EGFR in fibroblasts by PMA. The primary culture of dermal fibroblasts (TACE-Tg: $n=3$, WT: $n=3$) was treated by PMA at respective concentrations of 0, 20, 160, and 1300 nM. After 4 h of incubation at 37 °C, RNA was extracted from the cells, and then the expression of type I collagen (collagen 1A1) was examined by real-time RT-PCR (**a**). The fibroblasts derived from TACE-Tg mice were treated by 1300 nM of PMA with or without 25 μg/ml of TAPI-0 at 37 °C. After 4 h of incubation, RNA was extracted from the cells, and then the expression of type I collagen (collagen 1A1) was examined by real-time RT-PCR (**b**). The PMA-induced increase of type I collagen (collagen 1A1) was set as 100%. $^*P<0.05$. To determine the activation of EGFR, the expressions of EGFR and phosphorylated EGFR were examined (**c**). The primary culture of dermal fibroblasts was treated by PMA at respective concentrations of 0, 20, 160, and 1300 nM. After 1 h of incubation at 37 °C, RNA and cell lysates were extracted. The RNA was served for RT-PCR using the HPRT1 and EGFR primers. The lysates adjusted ranging from 10 to 40 μg/lane were fractionated on 7.5% SDS polyacrylamide gel, and then transferred onto PVDF membranes. After blocking by TBS-T containing 1% nonfat milk, the membranes were incubated with 1:2500 dilution of the anti-phosphorylated EGFR (p-EGFR) antibody overnight at 4 °C. After 3 times of wash by TBS-T, the membranes were next incubated with 1:25 000 dilution of the peroxidase-labeled secondary antibodies overnight at 4 °C. Protein bands were detected using ECL Advance Western Blotting Detection kit. As an internal control, the amount of actin was monitored by the anti-actin antibody. Experiments were repeated 3 times, and similar results were reproduced. Representative data are shown.

collagen using primary culture of dermal fibroblasts was examined in this study. Results indicated that PMA effectively activated TACE and subsequently increased expression of the type I collagen in the fibroblasts derived from TACE-Tg mice (Figure 7a). Furthermore, the induction of type I collagen by PMA was significantly inhibited by the TACE inhibitor (Figure 7b). These findings support our conclusion that TACE overexpression and activation in fibroblasts could contribute to dermal fibrosis. However, this does not necessarily mean that TACE exclusively regulates the PMA-induced type I collagen expression in dermal fibroblasts because TAPI-0 is not a specific inhibitor of TACE.

The substrates of TACE involved in the process of dermal fibrosis after the PMA-induced inflammation have not been identified. However, the amount of phosphorylated EGFR was increased by the PMA treatment of dermal fibroblasts (Figure 7c). As the expression of type I collagen could be driven by the EGFR signal,[12] TACE activated by PMA could shed off putative EGFR ligands on the surface of fibroblasts. Subsequently, the soluble EGFR ligands could bind and activate EGFR on fibroblasts through the autocrine and paracrine pathways and increase the type I collagen expression resulting in induction of dermal fibrosis. With regard to the EGF signaling pathway, EGFR ligands, including transforming growth factor-α (TGF-α), heparin-binding EGF (HB-EGF), amphiregulin, and epiregulin, may be the candidates shed by TACE. Among them, amphiregulin is known to be expressed in fibroblasts;[19] thus, this molecule is the next target in our continuing study.

The EGFR expression has been reported to be upregulated in dermal fibroblasts of SSc patients.[20] In the present study, the EGFR expression in TACE-Tg-derived dermal fibroblasts did not appear to be increased by PMA *in vitro*. This could be interpreted by the short duration of PMA stimulation (1 h stimulation) in the experiments. In addition, murine bleomycin-induced lung fibrosis could be suppressed by the EGFR tyrosine kinase inhibitor.[21] These findings suggest that the EGF signaling pathway comes to a great interest as the mechanism bridging the TACE expression and the pathogenesis of fibrosis.

In summary, the collective findings suggest the possibility that overexpression of TACE in fibroblasts could contribute to the pathogenesis of dermal fibrosis after inflammation. Further studies are needed to reveal the process leading to fibrosis; however, our data suggest that TACE and EGFR on fibroblasts may be novel therapeutic targets of dermal fibrosis, which is induced after diverse inflammatory disorders of the skin.

Supplementary Information accompanies the paper on the Laboratory Investigation website (http://www.laboratoryinvestigation.org)

DISCLOSURE/CONFLICT OF INTEREST
The authors declare no conflict of interest.

1. Black RA, Rauch CT, Kozlosky CJ, *et al.* A metalloproteinase disintegrin that releases tumour-necrosis factor-α from cells. Nature 1997;385: 729–733.

2. Moss ML, Jin SL, Milla ME, *et al.* Cloning of a disintegrin metalloproteinase that processes precursor tumour-necrosis factor-α. Nature 1997;385:733–736.
3. Van Wart HE, Birkedal-Hansen H. The cysteine switch: a principle of regulation of metalloproteinase activity with potential applicability to the entire matrix metalloproteinase gene family. Proc Natl Acad Sci USA 1990;87:5578–5582.
4. Grams F, Huber R, Kress LF, *et al.* Activation of snake venom metalloproteinases by a cysteine switch-like mechanism. FEBS Lett 1993;335:76–80.
5. Kang T, Zhao YG, Pei D, *et al.* Intracellular activation of human adamalysin 19/disintegrin and metalloproteinase 19 by furin occurs via one of the two consecutive recognition sites. J Biol Chem 2002;277:25583–25591.
6. Endres K, Anders A, Kojro E, *et al.* Tumor necrosis factor-α converting enzyme is processed by proprotein-convertases to its mature form which is degraded upon phorbol ester stimulation. Eur J Biochem 2003;270:2386–2393.
7. Doggrell SA. TACE inhibition: a new approach to treating inflammation. Expert Opin Investig Drugs 2002;11:1003–1006.
8. Shimizu M, Hasegawa N, Nishimura T, *et al.* Effects of TNF-α-converting enzyme inhibition on acute lung injury induced by endotoxin in the rat. Shock 2009;32:535–540.
9. Terao M, Murota H, Kitaba S, *et al.* Tumor necrosis factor-α processing inhibitor-1 inhibits skin fibrosis in a bleomycin-induced murine model of scleroderma. Exp Dermatol 2010;19:38–43.
10. Mohler KM, Sleath PR, Fitzner JN, *et al.* Protection against a lethal dose of endotoxin by an inhibitor of tumour necrosis factor processing. Nature 1994;370:218–220.
11. Maltzan K, Tan W, Pruett SB. Investigation of the role of TNF-α converting enzyme (TACE) in the inhibition of cell surface and soluble TNF-α production by acute ethanol exposure. PLoS One 2012;7:e29890.
12. Wu D, Peng F, Zhang B. Collagen I induction by high glucose levels is mediated by epidermal growth factor receptor and phosphoinositide 3-kinase/Akt signalling in mesangial cells. Diabetologia 2007;50: 2008–2018.
13. Ohta S, Harigai M, Tanaka M, *et al.* Tumor necrosis factor-α (TNF-α) converting enzyme contributes to production of TNF-α in synovial tissues from patients with rheumatoid arthritis. J Rheumatol 2001;28:1756–1763.
14. Moss ML, Sklair-Tavron L, Nudelman R. Drug insight: tumor necrosis factor-converting enzyme as a pharmaceutical target for rheumatoid arthritis. Nat Clin Pract Rheumatol 2008;4:300–309.
15. Bohgaki T, Amasaki Y, Nishimura N, *et al.* Up regulated expression of tumour necrosis factor α converting enzyme in peripheral monocytes of patients with early systemic sclerosis. Ann Rheum Dis 2005;64:1165–1173.
16. Leco KJ, Waterhouse P, Sanchez OH, *et al.* Spontaneous air space enlargement in the lungs of mice lacking tissue inhibitor of metalloproteinases-3 (TIMP-3). J Clin Invest 2001;108:817–829.
17. Mohammed FF, Smookler DS, Taylor SE, *et al.* Abnormal TNF activity in $Timp3^{-/-}$ mice leads to chronic hepatic inflammation and failure of liver regeneration. Nat Genet 2004;36:969–977.
18. Smookler DS, Mohammed FF, Kassiri Z, *et al.* Tissue inhibitor of metalloproteinase 3 regulates TNF-dependent systemic inflammation. J Immunol 2006;176:721–725.
19. Torring N, Sorensen BS, Bosch ST, *et al.* Amphiregulin is expressed in primary cultures of prostate myofibroblasts, fibroblasts, epithelial cells, and in prostate tissue. Prostate Cancer Prostatic Dis 1998;1:262–267.
20. Tokiyama K, Yokota E, Niho Y. Epidermal growth factor receptor of fibroblasts from patients with scleroderma. J Rheumatol 1990;17: 1463–1468.
21. Wang P, Tian Q, Liang ZX, *et al.* Gefitinib attenuates murine pulmonary fibrosis induced by bleomycin. Chin Med J (Engl) 2010;123:2259–2264.

RHEUMATOLOGY

Rheumatology 2013;52:523–528
doi:10.1093/rheumatology/kes310
Advance Access publication 28 November 2012

Concise report

Positive synovial vascularity in patients with low disease activity indicates smouldering inflammation leading to joint damage in rheumatoid arthritis: time-integrated joint inflammation estimated by synovial vascularity in each finger joint

Jun Fukae[1], Masato Isobe[1], Akemi Kitano[1], Mihoko Henmi[1], Fumihiko Sakamoto[1], Akihiro Narita[1], Takeya Ito[1], Akio Mitsuzaki[1], Masato Shimizu[1], Kazuhide Tanimura[1], Megumi Matsuhashi[1], Tamotsu Kamishima[2], Tatsuya Atsumi[3] and Takao Koike[3]

Abstract

Objective. To investigate the relationship between synovial vascularity and joint damage progression in each finger joint of patients with RA under low disease activity during treatment with biologic agents.

Methods. We studied 310 MCP and 310 PIP joints of 31 patients with active RA who were administered adalimumab (ADA) or tocilizumab (TCZ). Patients were examined with clinical and laboratory assessments. Power Doppler sonography was performed at baseline and at weeks 8, 20 and 40. Synovial vascularity was evaluated according to quantitative measurement. Hand and foot radiography was performed at baseline and at week 50.

Results. Composite scores of the DAS with 28 joints and the Simplified Disease Activity Index (SDAI) were significantly decreased from baseline to week 8, being sustained at a low level by biologic agents during the observational period. MCP and PIP joints with positive synovial vascularity after week 8 showed more subsequent joint damage progression than joints without synovial vascularity throughout the follow-up. The changes in radiographic progression in these joints were independent of the sum of synovial vascularity from baseline to week 40 or the occasional occurrence of positive synovial vascularity.

Conclusion. Smouldering inflammation reflected by positive synovial vascularity under low disease activity was linked to joint damage. The damage progressed irrespective of the severity of positive synovial vascularity. Even with a favourable overall therapeutic response, monitoring of synovial vascularity has the potential to provide useful joint information to tailor treatment strategies.

Trial registration. University Hospital Medical Information Network Clinical Trials Registry; http://www.umin.ac.jp/ctr/; UMIN000004476.

Key words: rheumatoid arthritis, power Doppler sonography, synovial vascularity, low disease activity.

CLINICAL

[1]Hokkaido Medical Center for Rheumatic Diseases, [2]Faculty of Health Science, Hokkaido University Graduate School of Health Science and, [3]Department of Medicine II, Hokkaido University Graduate School of Medicine, Sapporo, Japan.

Submitted 31 July 2012; revised version accepted 27 September 2012.

Correspondence to: Jun Fukae, Hokkaido Medical Center for Rheumatic Diseases, 1-45, 3-Chome, 1-Jo, Kotoni, Nishi-ku, Sapporo 063-0811, Japan. E-mail: jun.fukae@ryumachi-jp.com

Introduction

In RA, clinical evaluations for disease activity such as patients' symptoms, joint examinations and laboratory data do not have enough power to provide details on local joint inflammation [1]. To assess rheumatoid disease activity, composite scores such as the ACR core data set or the DAS with 28 joints (DAS28) have been developed to

compensate for the weak points in the use of a single clinical marker [2, 3]. Although these composite scores have been well established as disease activity markers, they cannot precisely predict the destruction of individual joints.

The appearance and increase in synovial vascularity related to vasodilation and angiogenesis indicates active joint inflammation [4]. Power Doppler sonography (PDS) enables visualization of synovial vascularity and numerical representation of local inflammation [5, 6].

We focused on the clinical significance of synovial vascularity in RA. We previously reported the prediction of the progression of local finger joint damage via early changes in synovial vascularity [7, 8]. Interestingly, we observed finger joints with persistence of synovial vascularity after achieving low disease activity. Here we report on the relationship between synovial vascularity and joint damage progression in two patient groups treated with different biologic agents, focusing on finger joints with positive synovial vascularity after achieving low disease activity.

Patients and methods

Patients

Thirty-one patients with RA who had started adalimumab (ADA) or tocilizumab (TCZ) therapies were analysed. The patients had been pre-treated with DMARDs [ADA: eight patients with MTX, one with tacrolimus (TAC), one with bucillamine (BUC) + TAC, one with MTX + TAC and one with SSZ + TAC; TCZ: nine patients with MTX, one with BUC and two with TAC] or pre-treated with biologic agents [ADA: one patient with MTX + infliximab (IFX); TCZ: three patients with MTX + IFX, one with MTX + etanercept and two with MTX + ADA]. Despite these treatment histories, all patients were refractory cases having at least one swollen joint in the MCP/PIP joints and a DAS28-ESR > 3.2. Demographic, clinical and laboratory characteristics of the patients are shown in Table 1. After baseline examinations, ADA was given to 13 patients and TCZ to 18 patients. The biologic agents were given according to the standard protocols (ADA 40 mg s.c. injection bi-weekly, TCZ 8 mg/kg i.v. infusion every 4 weeks). This study was conducted in accordance with the Declaration of Helsinki and was approved by the local ethics committee of Hokkaido Medical Center for Rheumatic Diseases. Informed consent was obtained from all patients before they entered the study.

Clinical examination

Swollen and tender joints and global assessment on a visual analogue scale (VAS) were assessed at baseline and at weeks 8, 20 and 40 by rheumatologists (J.F., M.S., M.M., K.T.) who were blinded to the ultrasonographic results. Blood tests for ESR and CRP were performed at each assessment.

Ultrasonography and assessment

Ultrasonography was performed at baseline and at weeks 8, 20 and 40 by one of three US experts (M.H., F.S., A.N.) specialized in musculoskeletal ultrasonography who were blinded to other clinical information. A linear array transducer (13 MHz) and ultrasonographic machine were used (EUP-L34P, EUB-7500, Hitachi, Tokyo, Japan). Power Doppler settings have been previously described [7, 8]. First to fifth MCP and first to fifth PIP joints were scanned in the longitudinal plane over the dorsal surface. The quantitative PDS method was established in a previous report [8]. A value of synovial vascularity was determined by counting the number of vascular flow pixels in the region of interest.

Radiography and assessment

Plain radiographs of hands, wrists and feet were obtained at baseline and at week 50. Radiological assessments were examined according to the Genant-modified Sharp score (GSS) by a rheumatologist (M.S.) who was blinded to other clinical information [9].

Statistical analysis

Differences of composite parameters were examined using the Student's *t*-test and other data were examined using a non-parametric test (Wilcoxon's signed-rank test and Mann–Whitney U test). Intra- and interobserver reliability of quantitative PDS were estimated by intraclass correlation coefficients (ICCs). The smallest detectable change for the radiographic score change was calculated according to a previous study [10]. $P < 0.05$ indicated statistical significance. Statistical analyses were calculated with the use of Excel (Microsoft, Redmond, WA, USA) and MedCalc 12.1.4.0 (MedCalc Software, Mariakerke, Belgium).

Results

Clinical disease activity

At baseline there were no significant differences of DAS28-ESR and SDAI between the ADA and TCZ groups (Table 1). In both groups these parameters were significantly decreased from baseline to week 8, followed by sustained low disease activity (ADA: $P = 0.0007$, $P = 0.0005$; TCZ: $P < 0.0001$, $P < 0.0001$, respectively) (Table 1).

Radiographic evaluation of joint damage

At baseline there were no significant differences in total GSS (TGSS) between the ADA and TCZ groups (Table 1). In both groups the TGSS increased significantly from baseline to week 50 ($P = 0.0122$, $P = 0.0181$, respectively).

Local GSS (LGSS) was evaluated in each finger joint. In the ADA group the median of the LGSS at baseline for MCP and PIP joints was 2 [interquartile range (IQR) 2–4] and 3 (IQR 1.5–4), respectively, and in the TCZ group the median of the LGSS at baseline for MCP and PIP joints was 3 (IQR 2–4) and 3 (IQR 2–4), respectively. The smallest detectable change values was calculated for the LGSS for single MCP and PIP joints [0.33, 0.31 less than the smallest unit of GSS scoring (0.5)].

TABLE 1 Clinical and laboratory characteristics of patients at baseline

	ADA	TCZ	*P*-value
Age, mean (range), years	53 (24-78)	56.4 (33-77)	0.516
Sex, female/male, *n*	12/1	18/1	
Duration of symptoms, median (IQR), months	62 (11-147)	142 (72-178)	0.156
ESR, median (IQR), mm/h	48 (34-54)	54 (34-64)	0.389
CRP, median (IQR), mg/dl	0.51 (0.09-0.89)	1.31 (0.24-3.03)	0.089
Swollen joint count, median (IQR)	3 (2-5)	5 (3-7)	0.179
Tender joint count, median (IQR)	5 (1-8)	4 (2-9)	0.984
Patient's global assessment by VAS, median (IQR)	50 (42-65)	67 (40-80)	0.544
Examiner's global assessment by VAS, median (IQR)	40 (40-50)	50 (33-70)	0.56
DAS28-ESR (S.D.)			
Baseline	5.03 (1.16)	5.28 (1.08)	0.575
Week 8	2.96 (0.86)	2.93 (0.81)	0.936
SDAI (S.D.)			
Baseline	21 (10.5)	24.7 (11.3)	0.275
Week 8	7.61 (5.48)	8.84 (4.31)	0.60
TGSS, median (IQR)			
Baseline	99.5 (73-116)	122.75 (98.75-160.75)	0.238
Week 50	108.5 (73-134.5)	125 (99.88-164.88)	0.271

Relationship between positive synovial vascularity and radiographic progression in finger joints

In the ADA group the mean and median of local synovial vascularity at baseline for the MCP and PIP joints were 197 and 0 (range 0-3053) and 218 and 0 (range 0-2414), respectively. In the TCZ group the mean and median of local synovial vascularity at baseline for the MCP and PIP joints were 416 and 0 (range 0-4686) and 167 and 0 (range 0-3195), respectively. Local synovial vascularity in both the ADA and TCZ groups decreased significantly from baseline to week 8 (ADA: MCP $P=0.0001$, PIP $P<0.0001$; TCZ: MCP $P=0.0002$, PIP $P=0.004$). We next categorized finger joints into four groups according to the occurrence of patterns of positive synovial vascularity: joints without synovial vascularity throughout the observational period [the negative (N) group], joints with positive synovial vascularity limited to the period from the baseline to week 8 [the therapeutic response (R) group], joints with intermittent occurrence of positive synovial vascularity in the observational period [the intermittently positive (IP) group] and joints with persistent positive synovial vascularity throughout the observational period [the persistently positive (PP) group]. Each patient had a different pattern of joints with positive synovial vascularity: patients in the N group (ADA $n=2$, TCZ $n=2$), patients in the R group (ADA $n=3$, TCZ $n=3$), patients in the IP or PP groups (ADA $n=3$, TCZ $n=6$) and patients in the mixed R and IP or PP groups (ADA $n=5$, TCZ $n=7$).

The change in the LGSS (ΔLGSS) of the R group showed no progression as compared with the N group or showed improvement of joint damage in the PIP joints of the ADA treatment group (Fig. 1). We next focused on the joints with positive synovial vascularity after week 8, comprising the IP and PP groups. These joints showed an increased ΔLGSS as compared with the N group (Fig. 1). The ΔLGSS between the IP and PP groups showed no significant difference with either ADA or TCZ treatment (Fig. 1).

To analyse the relationship between synovial vascularity and ΔLGSS in more detail in the joints comprising the IP and PP groups, we calculated the sum of synovial vascularity of each finger joint from baseline to week 40 to represent the total exposure to inflammation during the treatment period. The medians of the sum of synovial vascularity with ADA therapy for the MCP and PIP joints were 1456 (range 71-6352) and 1136 (range 71-4757), respectively. The medians of the sum of synovial vascularity with TCZ therapy for the MCP and PIP joints were 2947 (range 71-11289) and 1385 (range 71-5964), respectively. We categorized these joints into two groups: those with a sum of synovial vascularity $\leqslant$ median value [the low-level (L) group], and those with a sum of synovial vascularity $>$ median value [the high-level (H) group]. There were no significant differences in the ΔLGSS between the L group and H group with either ADA or TCZ treatment (Fig. 1).

Intra- and interobserver reliability for power Doppler ultrasonography

Representative PDS images for 20 MCP and 20 PIP joints were randomly chosen, and synovial vascularity was measured three times each by the three ultrasonographers (M.H., F.S. and A.N.). The obtained intraobserver ICC values were 0.997-0.999 for MCP joints and 0.998-0.999 for PIP joints. The interobserver ICC values were 0.992-0.996 for MCP joints and 0.991-0.999 for PIP joints.

Discussion

Our study revealed two noteworthy results. First, this study further emphasized a previous report [7] that early improvement and then disappearance of synovial vascularity resulted in reducing joint damage progression.

FIG. 1 Relationship between positive synovial vascularity and LGSS in finger joints.

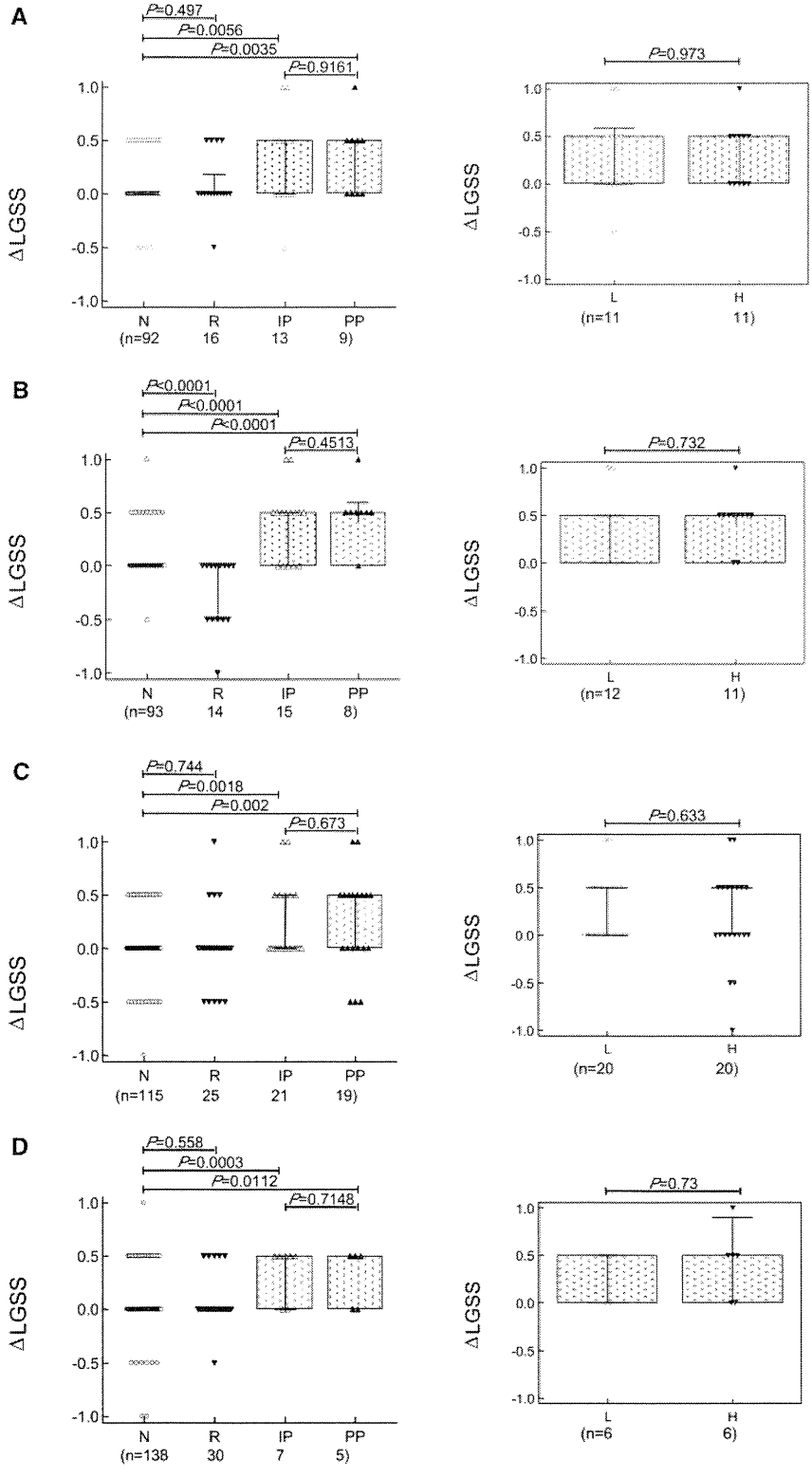

For ADA treatment, ΔLGSS of MCP (**A**) and PIP joints (**B**) is shown. For TCZ treatment, ΔLGSS of MCP (**C**) and PIP joints (**D**) is shown. Graphs on the left side show ΔLGSS of the N, R, IP and PP groups (Results section), which were categorized according to the occasional occurrence of positive synovial vascularity. For each joint in the IP and PP groups, the sum of synovial vascularity from baseline to week 40 was calculated and then categorized as L and H groups (Results section). Graphs on the right side show ΔLGSS of the L and H groups.

Secondly, a novel result was that persistence of positive synovial vascularity in local finger joints showed joint damage progression despite achieving low disease activity by biologic therapies. Interestingly, the ΔLGSS progressed independently of time-integrated joint inflammation estimated by the sum of synovial vascularity or occasional occurrence of positive synovial vascularity. These joints indicate the presence of low-level local joint inflammation, i.e. smouldering inflammation. The smouldering inflammatory joints could be categorized as a variation of subclinical synovitis described below.

Analysis of RA in the clinical remission phase revealed that there were asymptomatic or symptom-limited joints with poor prognosis. This joint inflammation or so-called subclinical synovitis can only be detected with imaging techniques [11–14]. The growing importance of imaging remission of rheumatoid activity has been confirmed, and imaging techniques such as joint ultrasonography have focused on detailed detection of local joint inflammation [15, 16].

Synovial vascularity detected by PDS is irrefutably linked to the level of joint inflammation [17, 18]. Naredo *et al.* [19] reported the correlation between time-integrated values of joint counts for positive synovial vascularity and total joint damage progression at 1 year. From these results, we speculated that increasing and persistent synovial vascularity might result in advanced joint damage progression; hence an increase in the occasional occurrence of positive synovial vascularity or the sum of synovial vascularity worsens the structural damage in smouldering inflammatory joints. Our data revealed that joints with positive synovial vascularity after week 8 (IP and PP groups) showed joint damage progression; however, their ΔLGSS progression did not relate to the occasional occurrence of positive synovial vascularity or the sum of synovial vascularity (Fig. 1). Accordingly, we concluded that the structural damage in joints with smouldering inflammation progressed independently of the level of the sum of synovial vascularity or the occasional occurrence of positive synovial vascularity. Importantly, the result might indicate that even low levels of positive synovial vascularity that occurred only once during the clinical improvement phase showed a risk for structural damage.

Although a correlation between the progression of systemic joint damage and time-integrated values of joint counts for positive synovial vascularity was reported [19], our study, which focused on synovitis and joint damage in individual finger joints, did not show such correlation. Whereas the previous study [19] showed the effect of non-biologic DMARDs, we studied biologic agents that rapidly improved acute inflammation. The DMARDs have slow therapeutic effect; thus the relationship between exposure to inflammation and joint damage progression may be closer in non-biologic DMARD users. Further, our data showed that some patients were in the mixed R and IP or PP group after starting biologic agents. This might indicate a discrepancy between overall therapeutic response and local joint response. Limitations of our study were its small scale and short observation period. Further larger studies are needed to confirm our observations.

In RA, tight control of joint inflammation is necessary for better outcomes. Treatment strategies should be changed according to the clinical response. Monitoring of synovial vascularity has the potential to provide useful joint information for daily practice and to tailor treatment strategies in RA.

Rheumatology key messages

- Finger joints with positive synovial vascularity under low disease activity showed structural deterioration in RA.
- Monitoring of synovial vascularity has the potential to provide useful information for daily practice in RA.

Disclosure statement: The authors have declared no conflicts of interest.

References

1 Jousse-Joulin S, d'Agostino MA, Marhadour T *et al.* Reproducibility of joint swelling assessment by sonography in patients with long-lasting rheumatoid arthritis (SEA-Repro study part II). J Rheumatol 2010;37:938–45.

2 Felson DT, Anderson JJ, Boers M *et al.* Preliminary definition of improvement in rheumatoid arthritis. Arthritis Rheum 1995;38:727–35.

3 Prevoo ML, van 't Hof MA, Kuper HH, van Leeuwen MA, van de Putte LB, van Riel PL. Modified disease activity scores that include twenty-eight-joint counts. Development and validation in a prospective longitudinal study of patients with rheumatoid arthritis. Arthritis Rheum 1995;38:44–8.

4 Koch AE. Review: angiogenesis: implications for rheumatoid arthritis. Arthritis Rheum 1998;41:951–62.

5 Newman JS, Adler RS, Bude RO, Rubin JM. Detection of soft-tissue hyperemia: value of power Doppler sonography. AJR Am J Roentgenol 1994;163:385–9.

6 Naredo E, Moller I, Cruz A, Carmona L, Garrido J. Power Doppler ultrasonographic monitoring of response to anti-tumor necrosis factor therapy in patients with rheumatoid arthritis. Arthritis Rheum 2008;58:2248–56.

7 Fukae J, Isobe M, Kitano A *et al.* Radiographic prognosis of finger joint damage predicted by early alteration in synovial vascularity in patients with rheumatoid arthritis: potential utility of power Doppler sonography in clinical practice. Arthritis Care Res 2011;63:1247–53.

8 Fukae J, Kon Y, Henmi M *et al.* Change of synovial vascularity in a single finger joint assessed by power Doppler sonography correlated with radiographic change in rheumatoid arthritis: comparative study of a novel quantitative score with a semiquantitative score. Arthritis Care Res 2010;62:657–63.

9 Genant HK, Jiang Y, Peterfy C, Lu Y, Redei J, Countryman PJ. Assessment of rheumatoid arthritis using

a modified scoring method on digitized and original radiographs. Arthritis Rheum 1998;41:1583–90.

10 Bruynesteyn K, Boers M, Kostense P, van der Linden S, van der Heijde D. Deciding on progression of joint damage in paired films of individual patients: smallest detectable difference or change. Ann Rheum Dis 2005;64: 179–82.

11 Peluso G, Michelutti A, Bosello S, Gremese E, Tolusso B, Ferraccioli G. Clinical and ultrasonographic remission determines different chances of relapse in early and long standing rheumatoid arthritis. Ann Rheum Dis 2011;70: 172–5.

12 Brown AK, Quinn MA, Karim Z *et al.* Presence of significant synovitis in rheumatoid arthritis patients with disease-modifying antirheumatic drug-induced clinical remission: evidence from an imaging study may explain structural progression. Arthritis Rheum 2006;54: 3761–73.

13 Filippucci E, Iagnocco A, Meenagh G *et al.* Ultrasound imaging for the rheumatologist VII. Ultrasound imaging in rheumatoid arthritis. Clin Exp Rheumatol 2007; 25:5–10.

14 Brown AK, Conaghan PG, Karim Z *et al.* An explanation for the apparent dissociation between clinical remission and continued structural deterioration in rheumatoid arthritis. Arthritis Rheum 2008;58:2958–67.

15 Saleem B, Brown AK, Keen H *et al.* Should imaging be a component of rheumatoid arthritis remission criteria? A comparison between traditional and modified composite remission scores and imaging assessments. Ann Rheum Dis 2011;70:792–8.

16 Dougados M, Devauchelle-Pensec V, Ferlet JF *et al.* The ability of synovitis to predict structural damage in rheumatoid arthritis: a comparative study between clinical examination and ultrasound. Ann Rheum Dis 2012. Advance Access published on 7 June 2012, doi:10.1136/annrheumdis-2012-201469.

17 Schirmer M, Duftner C, Schmidt WA, Dejaco C. Ultrasonography in inflammatory rheumatic disease: an overview. Nat Rev Rheumatol 2011;7:479–88.

18 Lainer-Carr D, Brahn E. Angiogenesis inhibition as a therapeutic approach for inflammatory synovitis. Nat Clin Pract Rheumatol 2007;3:434–42.

19 Naredo E, Collado P, Cruz A *et al.* Longitudinal power Doppler ultrasonographic assessment of joint inflammatory activity in early rheumatoid arthritis: predictive value in disease activity and radiologic progression. Arthritis Rheum 2007;57:116–24.

RHEUMATOLOGY

Rheumatology 2013;52:1775–1784
doi:10.1093/rheumatology/ket234
Advance Access publication 22 July 2013

Original article

Essential role of the p38 mitogen-activated protein kinase pathway in tissue factor gene expression mediated by the phosphatidylserine-dependent antiprothrombin antibody

Kenji Oku[1], Olga Amengual[1], Polona Zigon[2], Tetsuya Horita[1], Shinsuke Yasuda[1] and Tatsuya Atsumi[1]

Abstract

Objective. The aim of this study was to investigate the effects of phosphatidylserine-dependent antiprothrombin antibody (aPS/PT) on the expression of tissue factor (TF) and the signal transduction pathway in procoagulant cells.

Methods. Peripheral blood mononuclear cells (PBMCs) from a healthy donor, murine monocyte RAW264.7 cells and human umbilical vein endothelial cells (HUVECs) were treated with either IgG fractions obtained from APS patients who were positive for aPS/PT or a murine monoclonal aPS/PT antibody, 231D, in the presence of prothrombin. The levels of TF mRNA were measured using real-time PCR. TF function, as measured by procoagulant activity, was determined with a clotting assay. 231D binding on the surface of treated cells was determined by flow cytometric analysis. Screening for phosphorylation of intracellular signalling proteins was conducted using an array assay. Phosphorylation of p38 MAPK was quantitatively analysed with ELISA, and SB203580 was used as a specific inhibitor of p38 MAPK. Specific siRNA for p38 MAPK was used for the knockdown assay.

Results. The IgG fractions from APS patients and 231D induced TF mRNA overexpression and shortening of coagulation time in cells in the presence of prothrombin. The 231D moiety induced phosphorylation of p38 MAPK after binding to the cell surface of RAW264.7 cells. SB203580 or p38 siRNA significantly hampered TF overexpression.

Conclusion. Expression of TF in procoagulant cells was induced by aPS/PT via p38MAPK phosphorylation. This phenomenon may be correlated with the thrombogenicity of APS.

Key words: antiphospholipid syndrome, antiprothrombin antibody, tissue factor, p38 MAPK, procoagulant cell activation.

BASIC

Introduction

APS is a clinical condition characterized by recurrent thrombotic events and/or pregnancy morbidity associated with the persistence of aPLs. aPLs are a large and heterogeneous group of circulating immunoglobulins that appear either idiopathically or in a wide range of infectious or autoimmune diseases [1].

Traditionally aPLs are classified as aCLs, anti-beta-2-glycoprotein I (aβ_2GPI) antibodies or LA. Both aCL and aβ_2GPI are detected by ELISA, and both target the complex of β_2GPI and anionic phospholipids. These antibodies are designated β_2GPI-dependent anticardiolipin antibodies (aCL/β_2GPI) [2]. LA is detected by functional coagulation tests that require a careful and sequential series of examinations, and LA activities are indicative of the existence of heterogeneous antibodies, including aCL/β_2GPI.

[1]Department of Medicine II, Hokkaido University Graduate School of Medicine, Sapporo, Japan and [2]University Medical Centre, Department of Rheumatology, Ljubljana, Slovenia.

Submitted 2 November 2012; revised version accepted 15 May 2013.

Correspondence to: Kenji Oku, Department of Medicine II, Hokkaido University Graduate School of Medicine, N15 W7, Kita-ku, Sapporo 060-8638, Japan. E-mail: kenoku@med.hokudai.ac.jp

Evidence has shown that some LA activities depend on antibodies against prothrombin, which was first proposed as a possible cofactor for LA in 1959 [3]. The pathogenicity of aPT was reported from various institutes [4, 5]. Haj-Yahia *et al.* [6] reported that aPT obtained from mouse immunized with human prothrombin showed pathogenicity in an *ex vivo* model. However, association between antiprothrombin and clinical manifestation of APS is still a subject of controversy [7].

We showed that antibodies against the phosphatidylserine–prothrombin complex (aPS/PT), rather than antibodies against prothrombin alone, are closely associated with APS and LA [8], and their targeted antigen is a complex of anionic phospholipid and its binding protein, an analogue of the cardiolipin–β_2GPI complex. The sensitivity and specificity of aPS/PT for the diagnosis of APS have been assessed in a population with a variety of autoimmune disorders. It is now recognized that aPS/PT may have diagnostic potential, and they have been proposed as a candidate marker of APS and as an alternative test for LA [9–12].

In contrast to the clinical observation of a strong link between aPS/PT and thrombosis, only a few studies have demonstrated the thrombogenicity of aPS/PT. We have established a monoclonal aPS/PT, designated 231D, which specifically binds to phosphatidylserine–prothrombin complex (PS/PT) and possesses strong LA activity [13]. The concentration-dependent LA activity of the monoclonal aPS/PT and the epitope overlap reasonably represent the characteristics of autoimmune aPS/PT.

Tissue factor (TF) is the initiator of the extrinsic coagulation pathway, and we previously reported its upregulation in APS patients [14, 15]. Further, the results of our previous study and those of other studies demonstrated that monoclonal aCL/β_2GPI binds directly to procoagulant cells such as monocytes and endothelial cells (ECs), and that this binding mediates cell dysregulation, which may induce the clinical manifestations of APS [16–19]. When procoagulant cells are exposed to aCL/β_2GPI in the presence of β_2GPI, they produce thrombophilic molecules, particularly TF or adhesion molecules concomitant with activation of the p38 mitogen-activated protein kinase (MAPK) pathway [20–23]. Considering the analogy in the immunological aspects and clinical impact between aCL/β_2GPI and aPS/PT, these two populations of antibodies are likely to share in the pathophysiology of APS.

In this study we investigated the effects of aPS/PT on procoagulant cells by performing *in vitro* assays with purified IgG fractions obtained from the sera of patients with APS who were positive for aPS/PT and negative for aCL/β_2GPI, and with the monoclonal aPS/PT antibody, 231D.

Materials and methods

Monoclonal and autoimmune aPTs

Two murine monoclonal aPTs, 231D and 51A6, were previously established and characterized [13]. Briefly, the monoclonal aPS/PT antibody 231D was established as follows. BALB/c mice were intraperitoneally immunized with human prothrombin emulsified with complete or incomplete Freund's adjuvant. Spleen cells were fused with P3U1 mouse myeloma cells, and cells producing antibodies against PS/PT complex were screened using an aPS/PT ELISA, and the monoclonal antibody was sequentially purified by protein G-Sepharose affinity chromatography. 51A6, the monoclonal antibody directed against prothrombin, was established in the same manner as 231D with the exception of the immunogen used, prethrombin-1, which is a fragment of prothrombin lacking the phospholipid-binding site (Gla domain).

Both monoclonals bind strongly to the PS/PT complex, but not to phosphatidylserine alone; however, 231D has stronger binding to the PS/PT complex than 51A6. 51A6 binds to prothrombin coated on both irradiated and non-irradiated ELISA plates {antiprothrombin-alone (APT-A) activity [24]}; however, 231D shows little binding to prothrombin regardless of the plate type. 231D-spiked plasma has strong LA activity; 51A6-spiked plasma also has LA activity, but it is weaker. Binding of purified IgG from aPS/PT-positive patients with APS to the PS/PT complex is partially inhibited by 231D, but not by 51A6.

Therefore 231D has characteristics common to autoimmune aPS/PT. In contrast, 51A6 binding to prothrombin was not affected by the presence of phosphatidylserine, which is far different from the characteristics of the aPTs found in patients with APS.

IgG fractions were obtained from plasma samples of five APS patients with high titres of IgG aPS/PT in the absence of IgG aCL and aβ_2GPI using protein G-Sepharose affinity chromatography (MAbTrap-TMGII, Pharmacia). The patients included three females with a mean age of 46 (range 36–72) years, disease duration of 3–7 years and one to four past thrombotic events. IgG fractions from patients were pooled as the IgG aPS/PT fraction and frozen until use. Purified IgG fractions from plasma of three healthy individuals were prepared in the same fashion.

The study was performed in accordance with the Declaration of Helsinki and the principles of good clinical practice. Approval was obtained from the local ethics committee (Institutional Review Board of Hokkaido University Hospital), and informed consent was obtained from all subjects.

Cell isolation and preparation

Venous blood was collected from healthy donors into heparinized tubes. Peripheral blood mononuclear cells (PBMCs) were isolated by gradient centrifugation (Ficoll-Paque plus, GE Healthcare, Chalfont St Giles, Buckinghamshire, UK). The cells were then washed with Rosewell Park Memorial Institute (RPMI)-1640 medium (Sigma-Aldrich, St. Louis, MO, USA) supplemented with 10% heat-inactivated fetal calf serum (FCS; GIBCO BRL, Paisley, UK) containing penicillin and streptomycin, followed by centrifugation once at 400 *g* for 5 min at room temperature, and twice for 5 min at 4°C. The cells were then resuspended in RPMI-1640 and counted using the trypan blue dye exclusion method. The murine monocyte